



## Effect of BaO on physical, optical and structural characteristics of ZnO–Al<sub>2</sub>O<sub>3</sub>–B<sub>2</sub>O<sub>3</sub> glasses

H. A. Saudi<sup>1</sup>, S. U. EL Kameesy<sup>2</sup>, G. Mahmoud<sup>2</sup> and R. Saeed<sup>3</sup>

<sup>1</sup>Department of Physics, Faculty of Science (Girls' Branch), Al-Azhar University, Nasr City, Egypt.

<sup>2</sup>Department of Physics, Faculty of Science, Ain Shams University, Cairo, Egypt.

<sup>3</sup>Department of Physics, Faculty of Engineering, Misr International University (MIU), Cairo, Egypt.

### ABSTRACT

Zinc barium borate glasses with composition (65-x) B<sub>2</sub>O<sub>3</sub>-10Na<sub>2</sub>O-10Al<sub>2</sub>O<sub>3</sub>-10ZnO-5Li<sub>2</sub>O-xBaO with (0 ≤ x ≤ 40 % mol) have been prepared using melt quenching technique.

The density, molar volume and the optical absorption studies revealed that the optical band gap energy ( $E_{opt}$ ) and Urbach energy increase with the increase of BaO content. This is mainly due to the increased polarization of the Ba<sup>2+</sup> ions and the enhanced formation of non-bridging oxygen (NBO). The IR studies indicate that these glasses are made up of [AlO<sub>6</sub>], [BO<sub>3</sub>], [BO<sub>4</sub>], and [AlO<sub>4</sub>] basic structural units.

### Keywords

Borate glass, optical band energy, Structural properties.



## Council for Innovative Research

Peer Review Research Publishing System

Journal: JOURNAL OF ADVANCES IN PHYSICS

Vol. 11, No. 4

[www.cirjap.com](http://www.cirjap.com), [japeditor@gmail.com](mailto:japeditor@gmail.com)



## 1-Introduction

There has been an increasing interest in the synthesis, structure and physical properties of heavy metal oxide (HMO) glasses due to their high refractive index, high infrared transparency and high density [1]. Glasses based on heavy metal oxide such as BaO have wide applications in the field of glass ceramics, layers for optical and electronic devices, thermal and mechanical sensors, reflecting windows, etc. [1, 2]. Glass materials are one of the possible alternatives to concrete because they can be transparent to visible light and these properties can be modified by composition and preparation techniques. Binary alkali and alkaline borate glasses  $R_2O-B_2O_3$  ( $R = Li, Na, Ba, \text{etc.}$ ) have been studied extensively by several authors [2, 3]. Addition of BaO to borate network stabilizes the glasses [4,5]. The structure of the borate glasses is not a random distribution of  $[BO_3]$  triangles and  $[BO_4]$  tetrahedral, but a collecting, of these units to form well-defined and stable borate groups such as (diborate, triborate, tetraborate, etc.), that constitute the random three-dimensional network [6]. Borate glass is a suitable optical material for rare earth ions with high transparency, low melting point, high thermal stability and good rare earth ion solubility [7, 8]. The purpose of the present work is to study the dependence of several structural and optical properties on composition via infrared spectroscopy, optical spectroscopy and refractive index measurements.

## 2-Experimental techniques and theoretical calculation

The glass samples of the chemical composition  $(65-x) B_2O_3-10Na_2O-10Al_2O_3-10ZnO-5Li_2O-xBaO$  where  $(0 \leq x \leq 40 \text{ mol. \%})$  have been prepared from pure chemicals in a powder form by using the melt quenching technique. Each batch weights was melt in porcelain crucibles by placing them in an electric furnace for at least 2 hours, at  $1100^\circ C$  till a homogeneous mixture was formed. The molten mixture was quickly poured into preheated stainless steel mold. The quenched glasses were annealed at  $400^\circ C$  to reduce thermal stress, and cooled down to the room temperature. All glass samples were cut and polished in suitable shape for additional studies. The thickness of each sample was measured by a micrometer at room temperature.

The X-ray diffraction technique was used to check for possible crystallinity of the samples after quenching and annealing. XRD measurements were also performed, using Philips X-ray diffractometer PW/1710 with Cu-K $\alpha$  radiation with angle  $2\theta$  ranging from 10 to 80 degrees. The glass sample was used in the form of very fine homogeneous powder and a thin flat layer inserted in the path of X-ray beam. The air scattering was avoided by a suitable applied arrangement of XRD system. The receiving and divergence slits were properly chosen in both small and large  $2\theta$ -ranges, in order to improve the qualities of data collected as it could as it possible.

Densities of the samples were measured by using Archimedes principle with toluene as immersion liquid. The density was calculated by using the relation [9]

$$\rho = \frac{wt_a}{wt_a - wt_{liq}} \times \rho_{liq} \quad (1)$$

Where  $\rho$  is the density of glass sample,  $wt_a$  is weight of glass sample in air,  $wt_{liq}$  is weight of glass sample in toluene and  $\rho_{liq}$  is the density of toluene, ( $\rho_{liq} = 0.866 \text{ gm/cm}^3$  at room temperature).

The molar volume  $V_m$  is defined as the volume occupied by unit mass of the glass samples. The molar volume of a glass is given by the relation [10]

$$V_m = \sum (M/\rho) \quad (2)$$

Where  $M$  is the total molecular weight of the multi-component glass system.

FTIR measurement with a computer assisted double beam spectrophotometer (JASCO Corp., V-570, UV/VIS/NIR) was used to record the reflectance ( $R$ ) and transmittance ( $T$ ). The resolution limit of the spectrophotometer is equal to 0.5 nm. The accuracy of measuring reflectance and transmittance is  $\pm 0.002$ . The measurements were carried out at room temperature in the range (190-1500) nm. FTIR Measurements were performed for solid polished sample in the wavenumber range ( $4000-400 \text{ cm}^{-1}$ ) at room temperature using Vertex series FTIR spectrometer (Bruker optics), while the UV was measured by (JASCO V-570).

optical spectra over wide range of photon energy is very useful technique for understanding the basic mechanism of optically-induced transitions in crystalline and amorphous materials, as well as providing information about the band structure. Measurement of the optical absorption coefficient ( $\alpha$ ) near the fundamental absorption edge is particularly a standard method for the investigation of optically induced electronic transitions in many materials. The optical absorption coefficients ( $\alpha$ ) are evaluated from the optical transmittance ( $T$ ), reflectance ( $R$ ), and thickness " $t$ " of the samples using the relation:

$$\alpha = \frac{1}{t} \ln \left[ \frac{(1-R)}{T} \right] \quad (3)$$

Two types of optical transitions, (i.e. direct and indirect), occur at the absorption edge [11, 12]. Optical band gaps were calculated using absorption spectra for direct and indirect transitions for all prepared glass samples. The absorption coefficient,  $\alpha$ , as a function of the photon energy,  $E$ , can be described by the relation [13]

$$\alpha E = B (E - E_{opt})^n \quad (4)$$

Where ( $n=1/2$ ) the allowed transition,  $B$  is a constant and  $E_{opt}$  is the direct optical band gap. Relation (5) is also used for the indirect transitions. In that equation, ( $n=2$ ) the allowed transition,  $B$  is a constant and  $E_{opt}$  is indirect



optical band gap. For lower photon energies  $E$  lying between  $10^2$  and  $10^4 \text{ cm}^{-1}$ . The absorption coefficient characterizes as a function of Urbach energy can be expressed as follows:

$$\alpha = \alpha_0 \exp(E/\Delta E) \quad (5)$$

Where  $\alpha_0$  is a constant,  $E$  is the photon energy and  $\Delta E$  is the Urbach energy. The Urbach energy is interpreted as the width of the tail of the localized energy states in the band gap. The above relation can be expressed as follows:

$$\ln \alpha = (E/\Delta E) - \text{const} \quad (6)$$

The plots of natural logarithm of the absorption coefficient ( $\alpha$ ) versus photon energy ( $E$ ) are called Urbach plots. Urbach energy values ( $\Delta E$ ) were calculated by taking the reciprocals of the slopes of linear portion in the lower photon energy region of these curves as stated with relation (6) [14]

## 5– Results discussion

### 5.1. X-Ray diffraction analysis

The prepared glass samples were investigated by means of X-ray diffraction in order to confirm the amorphous state of the samples. The obtained XRD diffraction patterns are as shown in Fig.1. The displayed pattern confirms that the prepared samples are completely amorphous.

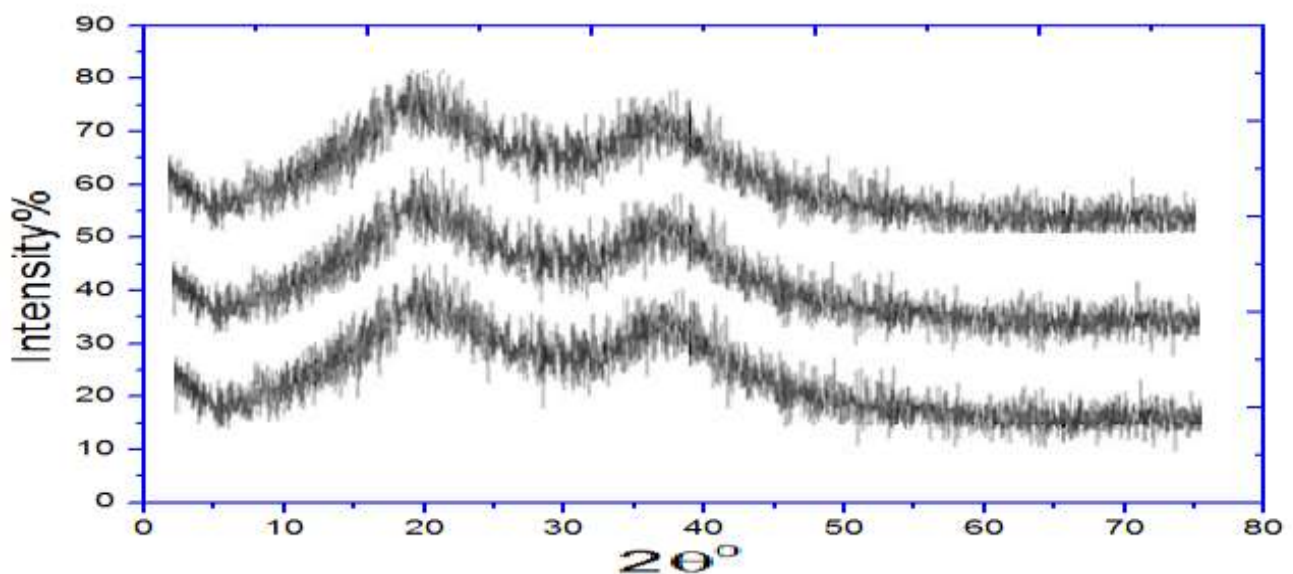


Fig. (1): XRD patterns at room temperature for three selected glass samples.

### 5.2-Density and Molar Volume

The density increases linearly with BaO content as has been illustrated in Fig. 2. The increase in the empirical density was also depicted in the same figure, for comparison. It is obvious that the empirical density values are higher than those obtained experimentally. This increase may be taken as evidence for the homogeneity of the glassy state of the prepared glass samples [15, 16 and 17].

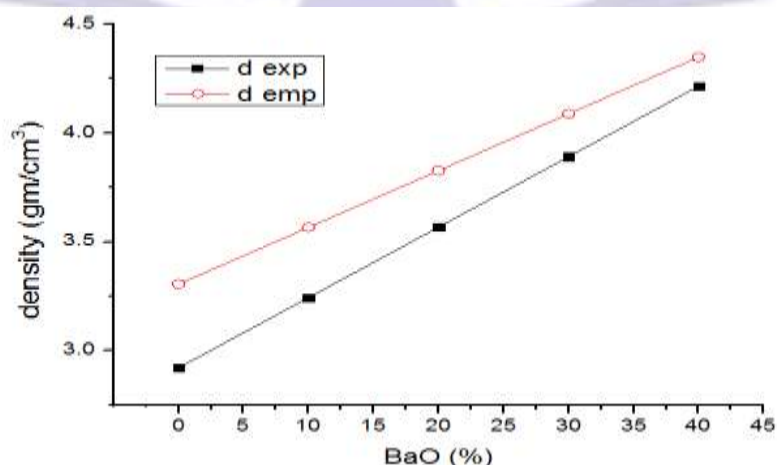


Fig. 2. Experimental and empirical densities versus BaO content

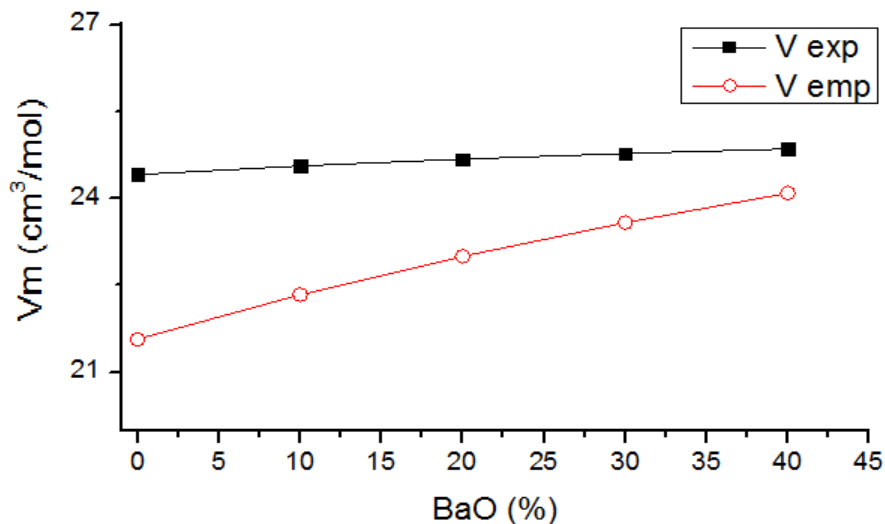


Fig. 3. Experimental and empirical  $V_m$  versus BaO content

The values of molar volume also increase linearly with BaO content in the glass system as shown in Fig. 3. It is obvious from this figure that the rate of increase of the  $(V_m)_{exp}$  is higher than that of the  $(V_m)_{emp}$ , which can be also taken as evidence for the homogeneity of the glassy state of the prepared glass samples. This increase in molar volume would have been possible only if BaO plays a role in the network formers. Thus, variation of molar volume in the present investigation suggests that the BaO are acting as network modifiers rather than network formers [18].

### 5.3- FTIR Study

Infrared spectroscopy has proved to be an important tool for the investigation of structure and dynamics of disorder materials. IR spectra of materials may help to get the idea of the nature of vibration in a disorder system [19]. The near-infrared region extending from 4000 to 2000  $\text{cm}^{-1}$  comprises the absorption bands due to vibrations of water, hydroxyl (OH) groups. The FTIR absorption spectra of all the glass samples are displayed in Fig. 4. The broad band at  $\sim 1398 \text{ cm}^{-1}$  can be attributed to B–O– stretching vibrations of  $\text{BO}_3$  units that exist in the form of various groups such as meta, pyro and ortho-borates [20]. The broadening of this peak indicates formation of pyro-borates at the expense of metaborates which in turn caused decrease in NBOs. The broad band  $\sim 861 \text{ cm}^{-1}$  may be due to combination of stretching vibrations of B–O bonds in tetrahedral  $\text{BO}_4$  units such as tri-, tetra-, pentaborate groups and vibrations of  $\text{AlO}_4$  structural units. [23] The  $\text{AlO}_4$  tetrahedrons may enter the glass network and alternate with  $\text{BO}_3$  units.

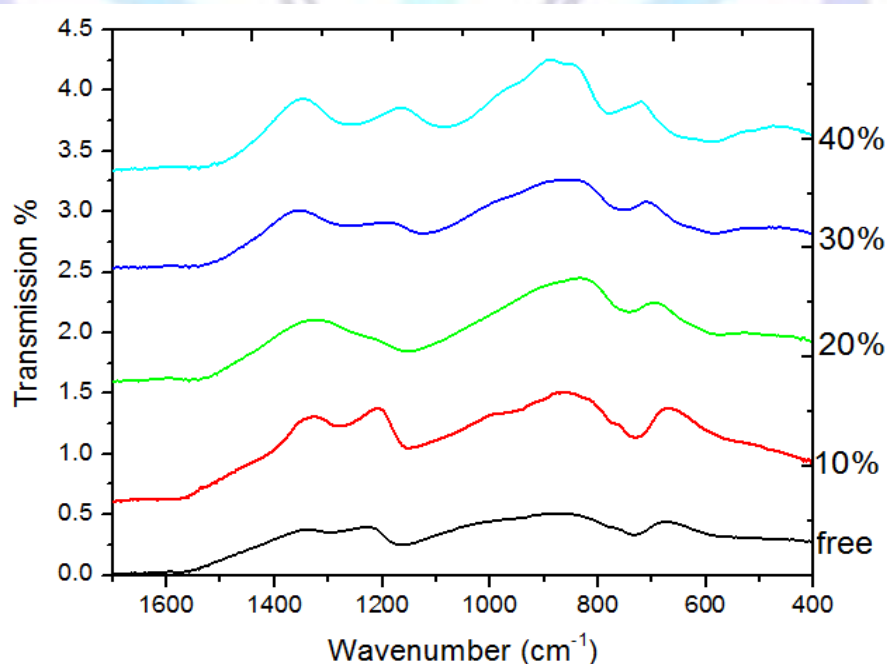


Fig.4: FTIR spectra of  $(65-x) \text{B}_2\text{O}_3\text{-}10\text{Na}_2\text{O-}10\text{Al}_2\text{O}_3\text{-}10\text{ZnO-}5\text{Li}_2\text{O-xBaO}$ , glass system.



The sharp absorption band  $\sim 690\text{ cm}^{-1}$  indicates B–O–B bending vibrations of borate network [20] and the vibration of bridged oxygen, which connects the two trigonal boron atoms [21]. The change in the coordination state of boron due to the change in modifier oxide content variation in the structural units  $\text{BO}_3$  triangles,  $\text{BO}_4$  tetrahedra, non-bridging oxygen atoms, and other structural groupings present in the glass network. The vibrational sub band due to  $\text{AlO}_6$  structural units is located at about  $452\text{ cm}^{-1}$ . [22]

#### 5.4-Optical Properties

Optical transmission spectra as a function of BaO concentration at room temperature in the wave length region 200 - 2600 nm are shown in Fig 5. Due to the homogeneous distribution of BaO in the prepared glass matrices, all glass samples are transparent. The optical transmission edge is not sharp and extended over wide wavelength range, in consistence with the amorphous nature of the prepared glasses.

From eq.5, by plotting  $(\alpha E)^{1/2}$  and  $(\alpha E)^2$  as a function of photon energy (E) Figs.6 and 7. The optical band gaps for indirect and direct transitions could be found. The respective values of  $E_{\text{opt}}$  were obtained by extrapolating to  $(\alpha E)^{1/2} = 0$  for indirect transitions and  $(\alpha E)^2 = 0$  for direct transitions [23]. From the Figs. it is clear that the absorption edges were not sharp which is an indication of amorphous nature of the samples. The increase in optical band gap in the present glass system indicates decrease in nonbridging oxygen content since the bridging oxygen (BOs) atoms are less excited than NBOs. Hence, with increasing BaO content in the glass, the number of non-bridging oxygen ions decreased [24]. The increment in optical band values means that there are less tails in the localized states. The variation in the optical bands with increasing BaO in the glass matrix is small and therefore rigorous structural changes might have not occurred in the glass network as has been illustrated in Figs. 8, 9 and table 1.

The values of Urbach energies ( $\Delta E$ ) for all test glasses were calculated by taking the reciprocals of the slopes of the linear portion in the lower photon energy regions of  $\ln \alpha$  versus E (hU) as shown in Fig. 10. The obtained result concerning the optical band gaps for direct and indirect transitions and the Urbach energies are given in table 1. The optical band gaps for direct transitions of the samples vary between 4.609–4.834 eV and vary between 3.135–3.219 eV for indirect transitions and the value of the width of the tails of localized states ( $\Delta E$ ) varied between 0.231 and 0.927 eV.

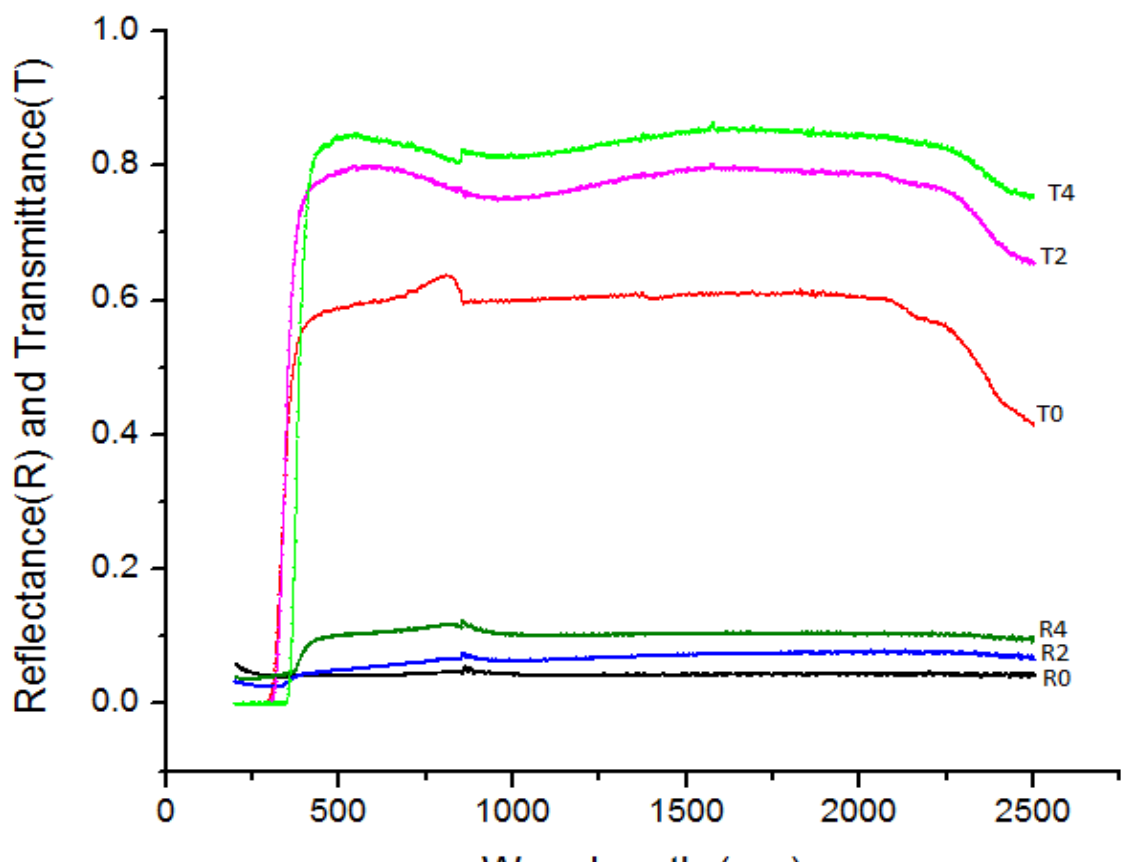


Fig.5:Optical transmission spectra of three selected glass samples.

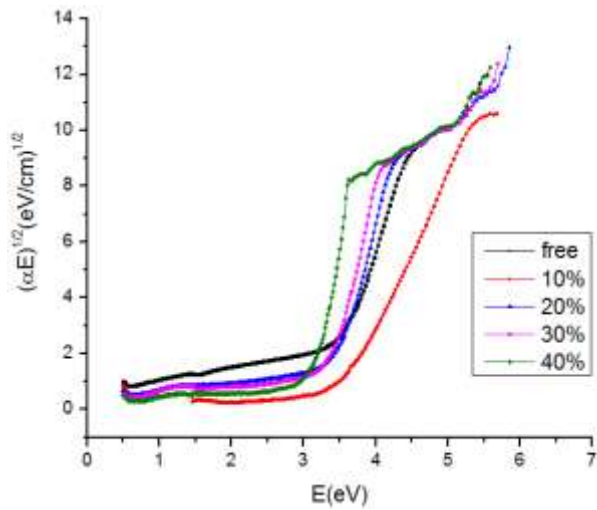


Fig.6:  $(\alpha E)^{1/2} \sim E$  variations of glass samples.

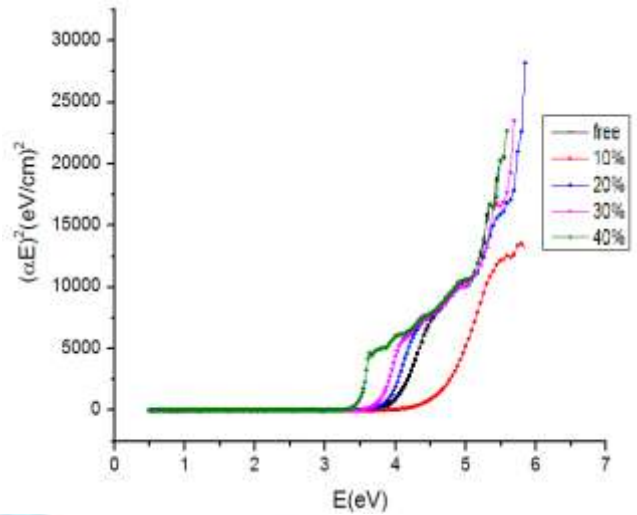


Fig.7:  $(\alpha E)^2 \sim E$  variations of glass samples.

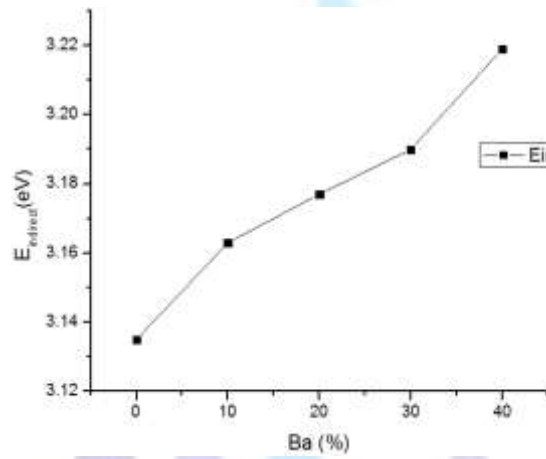


Fig.8: indirect  $E_g \sim Ba\%$ .

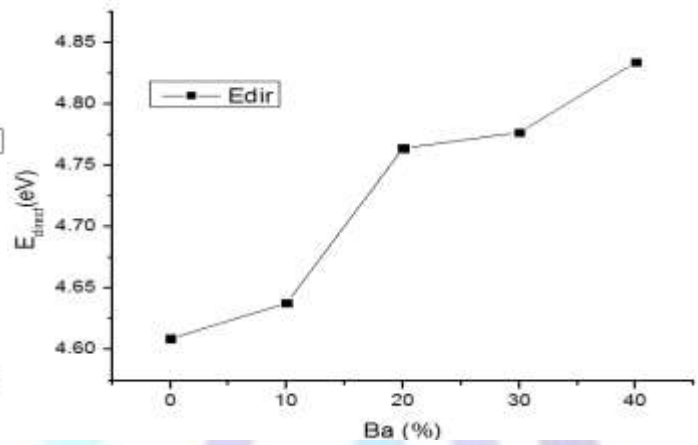


Fig. 9: direct  $E_g \sim Ba\%$ .

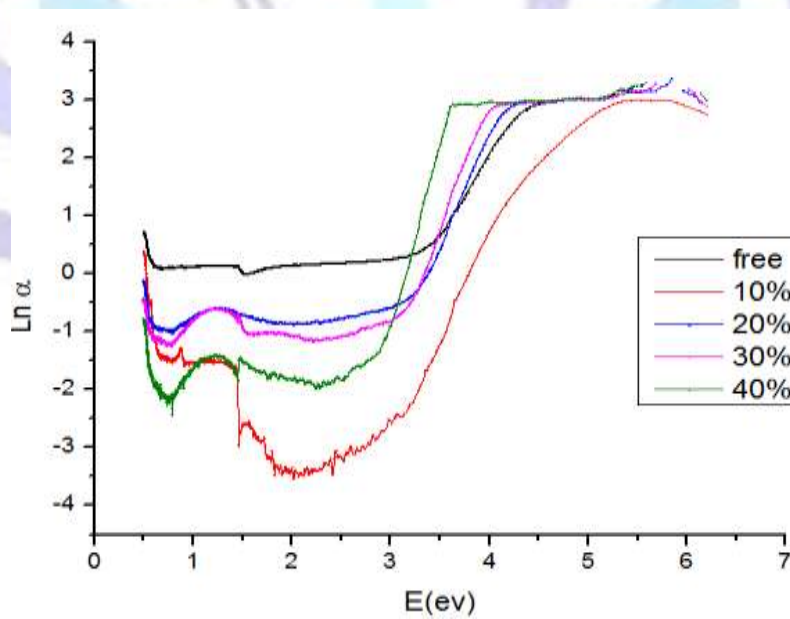


Fig.10:  $\ln(\alpha) \sim E$  variations of glass samples.

**Table 1. Direct and indirect optical band gaps, Urbach energies of glass samples.**

Sample no.	E <sub>opt</sub> (direct) (eV)	E <sub>opt</sub> (indirect) (eV)	ΔE (eV)
1	4.609	3.135	0.389
2	4.638	3.163	0.231
3	4.764	3.177	0.631
4	4.777	3.190	0.681
5	4.834	3.219	0.927

## CONCLUSION

(65-x) B<sub>2</sub>O<sub>3</sub>-10Na<sub>2</sub>O-10Al<sub>2</sub>O<sub>3</sub>-10ZnO-5Li<sub>2</sub>O-xBaO with (0 ≤ x ≤ 40 % mol.), glasses have been prepared and their optical properties are investigated. Densities and energy bandgaps are discussed in terms of the glass composition and structure. From the present obtained data it is clear that as BaO content increased both the density and molar volume values increased. The comparison between the experimental and empirical density and molar volume values proved that all the glass samples are in amorphous glassy phase. FTIR spectra of the present glass system indicate that B<sub>2</sub>O<sub>3</sub> and Al<sub>2</sub>O<sub>3</sub> acts as network former and exists in mainly [BO<sub>3</sub>] and [AlO<sub>4</sub>] structural groups, where BaO acts as glass network modifiers. The increase in the optical band gap in the present glass system indicates decrease in non-bridging oxygen content since the bridging oxygen (BOs) atoms are less excited than NBOs. Hence, with the increase in BaO content in the glass, the number of non-bridging oxygen ions decreased.

## References

- [1] H. A. Saudi, A.G. Mostafa, N. Sheta, S.U. ElKameesy and H.A. Sallam, *Physica B: Physics of Condensed Matter* 406 (2011) pp. 4001-4006.
- [2] H. A. Saudi, *Applied Mathematics and Physics*, (2013), Vol. 1, No. 4, 143-146 (<http://pubs.sciepub.com/amp/1/4/7> © Science and Education Publishing) .
- [3] E. I. Kamitsos and M. A. Karakassides, *Physics and Chemistry of Glasses*, vol. 30, no. 1, pp. 19–26, 1989.
- [3] E. I. Kamitsos, M. A. Karakassides, and G. D. Chryssikos, *Physics and Chemistry of Glasses*, vol. 30, no. 6, pp. 229–234, (1989).
- [4] H. A. Saudi, *SOP TRANSACTIONS ON APPLIED PHYSICS*, Vol. 1, (2014), no. 1.
- [5] K.K. Mahato, S.B. Rai, Anitha Rai, *Spectrochim. Acta, Part A* 60 (2004) 979 – 985.
- [6] K. Marimuthu, R.T. Karunakaran, S. Surendra Babu, G. Muralidharan, S. Arumugam, C.K. Jayasankar, *Solid State Sci.* 11 (2009) 1297 – 1302.
- [7] Hai Lina, Dianlai Yang, Guishan Liu, Tiecheng Ma, Bin Zhai, Qingda An, Jiayou Yu, Xiaojun Wang, Xingren Liu, Edwin Yue-Bun Pun, *J. Lumin.* 113 (2005) 121–128.
- [8] B. Deva Prasad Raju, C. Madhukar Reddy, *Opt. Mater.* 34 (2012) 1251 – 1260.
- [9] S. R. Manohara et al, *Journal of the Korean Physical Society*, Vol. 59, No. 2, (2011), 2039–2042.
- [10] Singh, K.J., Singh, N., Kaundal, R.S., Singh, K., *Nucl. Instrum. Methods B* 207, (2008) 944–948.
- [11] Altaf, M., Chaudhry, M.A., Zahid, M., *Journal of Research (Science)*, Bahauddin Zakariya University, 14(2): 253-259 (2003).
- [12] Mott, N.F., Davis, E.A., "Electronic Processes in Non-Crystalline Materials", Clarendon Pres, Oxford (1971)
- [13] Mott, N.F., Davis, E.A., "Electronic Processes in Non-Crystalline Materials", Clarendon Pres, Oxford (1979)
- [14] Subrahmanyam, K., Salagram, M., *Opt. Mater.*, 15: 181-186 (2000).
- [15] S. Sindhu, S. Sanghi, A. Agarwal, S. Sonam, V. P. Seth, and N. Kishore, *Physica B*, vol. 365, no. 1–4, pp. 65–75, 2005.
- [16] N. P. Lower, J. L. McRae, H. A. Feller et al., *Journal of Non-Crystalline Solids*, vol. 293–295, no. 1, pp. 669–675, 2001..
- [17] B. C. Sales and L. A. Boatner, in *Radioactive Waste Forms for the Future*, Chapter 3, ed. by Werner Lutze and R. C. Ewing, Elsevier North-Holland, Amsterdam, 1988.



- [18] M. Ganguli and K. J. Rao, *Journal of Solid State Chemistry*, vol. 145, no. 1, pp. 65–76, 1999. [View at Publisher](#) · [View at Google Scholar](#) · [View at Scopus](#)
- [19] P. Becker, *Crystal Research and Technology*, Vol. 38, No. 1, 2003, pp. 74-82. doi:10.1002/crat.200310009.
- [20] B. Sumalatha, I. Omkaram, T. R. Rao, and C. L. Raju, *Journal of Non-Crystalline Solids*, vol. 357, no. 16-17, pp. 3143–3152, (2011).
- [21] E. I. Kamitsos, "Infrared Studies of Borate Glasses," *Glass Physics and Chemistry*, Vol. 44, (2003), 79-87.
- [22] D. Muller, G. Berger, I. Grunze, G. Ladwig, E. Hallas and U. Haubenreisser, *Phys. Chem. Glasses* 24
- [23] Chakradhar, R.P.S., Ramesh, K.P., Rao, J. L., Ramakrishna, J., *J. Phys. Chem. Solids*, 64: 641-650 (2003).
- [24] S. Sanghi, S. Sindhu, A. Agarwal, and V. P. Seth, *Radiation Effects and Defects in Solids*, vol. 159, no. 6, pp.369–379, (2004).

